

Understanding and Mitigating Packet Corruption in Data Center Networks

Danyang Zhuo
University of Washington

Monia Ghobadi
Microsoft Research

Ratul Mahajan
Microsoft Research & Intentionet

Klaus-Tycho Förster
Aalborg University

Arvind Krishnamurthy
University of Washington

Thomas Anderson
University of Washington

ABSTRACT

We take a comprehensive look at packet corruption in data center networks, which leads to packet losses and application performance degradation. By studying 350K links across 15 production data centers, we find that the extent of corruption losses is significant and that its characteristics differ markedly from congestion losses. Corruption impacts fewer links than congestion, but imposes a heavier loss rate; and unlike congestion, corruption rate on a link is stable over time and is not correlated with its utilization.

Based on these observations, we developed CorrOpt, a system to mitigate corruption. To minimize corruption losses, it intelligently selects which corrupting links can be safely disabled, while ensuring that each top-of-rack switch has a minimum number of paths to reach other switches. CorrOpt also recommends specific actions (e.g., replace cables, clean connectors) to repair disabled links, based on our analysis of common symptoms of different root causes of corruption. Our recommendation engine has been deployed in over seventy data centers of a large cloud provider. Our analysis shows that, compared to current state of the art, CorrOpt can reduce corruption losses by three to six orders of magnitude and improve repair accuracy by 60%.

CCS CONCEPTS

• **Networks** → *Network measurement; Network reliability; Data center networks; Network management;*

KEYWORDS

CorrOpt, Packet Corruption, Data Center Networks, Optics, Fault Mitigation

ACM Reference format:

Danyang Zhuo, Monia Ghobadi, Ratul Mahajan, Klaus-Tycho Förster, Arvind Krishnamurthy, and Thomas Anderson. 2017. Understanding and Mitigating Packet Corruption in Data Center Networks. In *Proceedings of SIGCOMM '17, Los Angeles, CA, USA, August 21–25, 2017*, 14 pages. <https://doi.org/10.1145/3098822.3098849>

Permission to make digital or hard copies of all or part of this work for personal or classroom use is granted without fee provided that copies are not made or distributed for profit or commercial advantage and that copies bear this notice and the full citation on the first page. Copyrights for components of this work owned by others than ACM must be honored. Abstracting with credit is permitted. To copy otherwise, or republish, to post on servers or to redistribute to lists, requires prior specific permission and/or a fee. Request permissions from permissions@acm.org.

SIGCOMM '17, August 21–25, 2017, Los Angeles, CA, USA

© 2017 Association for Computing Machinery.

ACM ISBN 978-1-4503-4653-5/17/08...\$15.00

<https://doi.org/10.1145/3098822.3098849>

1 INTRODUCTION

Packet losses in data center networks (DCNs) hurt applications and can lead to millions of dollars in lost revenue [20, 26, 37]. For instance, packet loss rate above 0.1% causes RDMA's throughput to drop by 25% for bulk transfer [36]. For user-facing video traffic, loss rates of 0.01% can cause TCP CUBIC's throughput to drop by 50% [10]. Even sporadic packet losses can cause catastrophic virtual machine reboots [5].

Consequently, researchers have explored several approaches to reduce packet loss, including congestion control, active queue management, load balancing, and traffic engineering [2–4, 12, 28, 31, 32, 36]. All of these approaches, however, focus on one source of packet loss—congestion that occurs when the network's load exceeds its capacity.

However, another significant source of packet loss, namely packet corruption, has received little attention. Packet corruption occurs when the receiver cannot correctly decode transmitted bits. Such decoding errors cause the cyclic redundancy check in the Ethernet frame to fail and force the receiver to drop the packet. While recent studies categorize different sources of packet loss and acknowledge packet corruption as a contributor [5, 34, 37], not much is known today about the extent and characteristics of corruption-induced packet loss.

This paper presents what to our knowledge is the first large-scale study of packet corruption in DCNs. We monitor 350K switch-to-switch, optical links within 15 data centers of a major cloud provider, over seven months. We find that, despite the cloud provider's efforts to mitigate corruption, the number of packets lost due to corruption is significant. To improve mitigation techniques for packet corruption, we need a thorough understanding of its characteristics. We uncover several relevant characteristics of corruption losses and contrast them with those of congestion. For instance, while the loss rate due to congestion varies with link utilization, that due to corruption is relatively stable over time and is independent of the link's utilization. This observation implies that reducing the load on the link, as in congestion control, will not reduce packet corruption rate. We also find that, compared to congestion, corruption plagues fewer links but imposes higher loss rates on those links. Finally, we find that corruption exhibits weak locality, i.e., the chances of multiple corrupting links being on the same switch or being topologically close are noticeable but low, while congestion exhibits strong locality.

We also analyze hundreds of trouble ticket logs to find the common root causes of corruption. These range from faulty transceivers (i.e., devices that convert between optical and electrical signals) and switches, to poorly installed hardware, to damaged optical fiber, to

dirty optical connectors. By monitoring the optical layer contemporaneously with the tickets, we uncover the common symptoms for each such root cause.

The prevalent method to mitigate corruption is to disable links with corruption loss rate above a certain level (e.g., 10^{-6}), provided that the switches to which they attach have at least a threshold number of active uplinks toward the spine of the DCN [26]. This threshold ensures that the hosts using the switch have enough left-over capacity—otherwise, we might replace corruption losses with heavy congestion losses. Links are disabled automatically using software that monitors the corruption loss rate of each link. Though it does not *repair* corrupting links, this software is important because it reduces the chances of application traffic experiencing corruption losses. For each disabled link, a maintenance ticket is issued for operators to manually repair the link. The operators attempt to repair the link via a sequence of steps (e.g., clean the optical fiber and connectors; replace the transceiver; replace the cable), based on their expertise and largely independent of the root cause. The link is enabled after each step, and the next step is taken if the previous one did not succeed at eliminating corruption.

The method above has two limitations. First, the criterion for disabling links is greedy and local. While such decisions can be made quickly, they miss better opportunities that can reduce the level of corruption losses, i.e., disable links with higher corruption rates or disable more corrupting links. We show that such opportunities exist while meeting the same capacity constraint. Second, since the strategy to repair corruption is agnostic of the root cause, it can take multiple steps to eliminate corruption. In fact, with the current strategy, the link is fixed in the first step only 50% of the time.

Based on the observations above, we develop CorrOpt, a system to mitigate corruption in DCNs. Because the problem of identifying the optimal set of corrupting links to disable, which minimizes corruption losses while meeting capacity constraints, is NP-hard, CorrOpt uses a two-phase approach. First, when a link starts corrupting packets, a fast decision is made on whether the link can be safely turned off. Even this fast decision allows us to lower corruption losses than the current method because it considers the entire set paths from top-of-rack switches to the spine, instead of just the switches adjacent to the link. But this fast decision is not optimal. To approximate optimality, we use a second phase that does a global optimization to determine the set of links that can be safely disabled. The combination of the two phases allows us to react quickly and optimize later.

CorrOpt also has a recommendation engine that uses a root cause-aware approach to propose the right repair for corrupting links. Based on the link’s characteristics (i.e., corruption rate, optical transmit power, optical receive power) and history of actions taken thus far (if any), it generates concrete recommendations for operators on what corrective action is needed. This recommendation engine has been deployed in over 70 DCNs of our cloud provider.

We evaluate CorrOpt using the deployment of the recommendation engine and a trace-based analysis using data from production DCNs. We find that CorrOpt responds to packet corruption quickly and lowers the amount of corruption losses by up to three to six orders of magnitude, while meeting the desired capacity constraints. We also find that our recommendation engine has improved the accuracy of repairing the link at the first attempt from 50% to 80%.

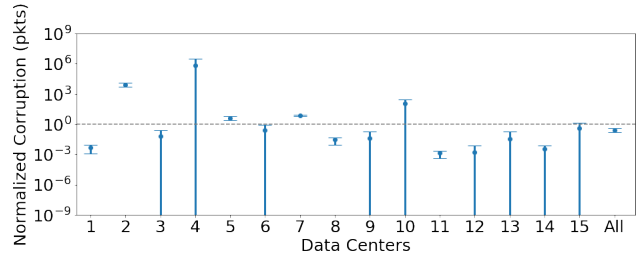


Figure 1: Mean and standard deviation of packets lost per day due to corruption across 15 DCNs, sorted by their size. Values are normalized by the mean number of congestion losses in each DCN. Horizontal dashed line denotes the threshold when packets loss due to corruption and congestion are the same. In most cases, corruption and congestion losses are on par.

2 EXTENT OF PACKET CORRUPTION

We demonstrate the need to understand and mitigate packet corruption by quantifying its extent in today’s DCNs. We show that the number of packets lost due to corruption is startlingly high.

Our analysis considers corruption- and congestion-induced losses in 15 production data centers. We focus on switch-to-switch links. Corruption mitigation, by disabling or routing around corrupting links, is relevant only for such links, not server-to-ToR links. Further, as we discuss later, the complexity of repair is a concern only for switch-to-switch links, which are optical and can go long distances; server-to-ToR links, which are electrical and short, simply get replaced. As the data centers that we study use standard designs and physical layer technologies (e.g., transceivers, fibers), we expect our findings to be applicable to other data centers as well.¹

The DCNs in our study have 4–50K links, and the total across all of them is 350K. For each link, we use SNMP [11] to query its packet drop, packet error, and total packet counts, as well as its optical power levels every 15 minutes. Our network operators found SNMP to be a reliable and lightweight mechanism for monitoring these counters. The data cover a period of seven months. The results in this section are based on three weeks of data, and the next section looks deeply into one representative week. The rest of the paper uses the entire data set.

Figure 1 shows the number of packets lost per day due to packet corruption and congestion. The DCNs are sorted by size. For confidentiality, the number of packet losses on the Y-axis is normalized with respect to mean congestion per DCN. The error bars represent the standard variation around the mean for packets lost due to corruption on different days.

We see that, while results vary across data centers and days, in aggregate, the number of corruption losses is on par with congestion losses on the switch-to-switch links that we study. (Results for server-attached links may differ.) In other words, for every congestion loss that applications experience, they will experience a corruption loss. Although this graph does not show corruption *rate*,

¹Our data centers have diverse ages and have been through different rounds of equipment replacement cycles. We do not have data of when each device is installed and thus cannot study the effect of packet corruption over device lifetime.

Loss bucket	links w. corruption	links w. congestion
$[10^{-8} - 10^{-5})$	47.23%	92.44%
$[10^{-5} - 10^{-4})$	18.43%	6.35%
$[10^{-4} - 10^{-3})$	21.66%	0.99%
$[10^{-3} +)$	12.67%	0.22%
total	100%	100%

Table 1: Comparison of the normalized distribution of links with congestion and corruption loss for different loss buckets. 12.67% of total links that experience corruption, have a corruption loss rate greater than or equal to 10^{-3} (0.1% loss rate) whereas only 0.22% of links with congestion, have congestion loss rate of 10^{-3} . The numbers in each column are normalized so that the table does not reveal the overall percentage of links with congestion or corruption losses for confidentiality reasons.

the next section shows that it can be quite high for some links. This high level of corruption loss happens even though there is already a system to discover and turn off links with corruption. While this system has limitations, which we explain in §5, we estimate that without it, corruption-induced losses would be two orders of magnitude higher.

Our results clearly demonstrate the need for an effective strategy to mitigate corruption in DCNs. Our proposed system, CorrOpt, provides such a strategy. To explain the rationale underlying its design, in the next two sections, we dig more deeply into the nature of corruption and its root causes.

3 CORRUPTION CHARACTERISTICS

To develop a thorough understanding of packet corruption, in this section we identify the characteristics of corruption and compare them to congestion. Though not our focus, our observations can also help load balancing and congestion control systems appropriately handle congestion vs. corruption losses when switch counters are not available to distinguish the two.

Corruption impacts fewer links but can be more severe than congestion. Our data reveal that while congestion is a more widespread phenomenon in terms of the links it impacts, packet corruption affects fewer links. We compute the percentage of links with congestion and corruption loss rate above 10^{-8} and find that the total number of links with corruption is less than 2-4% of those with congestion.²

This difference suggests that a small set of links have high corruption loss rate, given that the number of corruption and congestion losses is similar. Table 1 shows the distribution of links with corruption and congestion in different loss buckets, normalized such that the total in each column adds to 100%. Overall, only a small percentage of links in the DCN have any corruption or congestion; we exclude these percentages for confidentiality. We see that over 90% of links with congestion have a loss rate between 10^{-8} and 10^{-5} .

²IEEE 802.3 standard requires each link to have corruption loss rate under 10^{-8} , but operators today tend to worry only when packet loss rates start approaching 10^{-6} . In this paper, we conservatively use 10^{-8} as the threshold to deem a link as lossy or non-lossy.

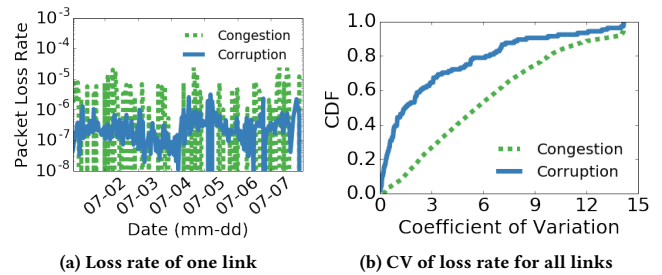


Figure 2: Corruption loss rate is more stable over time than congestion loss rate. 2a compares the corruption loss rate with congestion loss rate of a link for one week and shows corruption has little variation than congestion. 2b plots the CDF of the coefficient of variance of packet loss rate across 15 data centers for one week and shows corruption loss rate has less variation compared to congestion loss rate.

As the loss rate increases, the percentage of links with congestion in each category decreases. This is expected, as congestion control reduces flows' sending rate which lowers the loss rate. However, the same trend does not hold for corruption: 12.67% of links appear in the last loss bucket with loss rate $\geq 10^{-3}$ (or 0.1%) whereas congestion appears in 0.22% of links.

Corruption rate is stable over time. Figure 2a shows the corruption and congestion loss rate of example links for one week. We can see that the corruption rate has less variation compared to congestion which varies by three orders of magnitude in a short amount of time. A similar observation holds for the entire data set. We quantify the level of variation of loss rate on a link using the coefficient of variation (CV), which is standard deviation divided by the mean.

Figure 2b shows the CDF of CV between congestion and corruption loss rates for all links in one week. For 80% of the links, CV for corrupting links is smaller than four while for congestion, it is more than twice that amount. Thus, for most links, corruption loss rate is more stable than congestion loss rate.

Corruption rate is uncorrelated with utilization. Inherently, corruption loss rate is stable over time because it does not vary with link utilization. Figure 3a shows a scatter plot of utilization versus loss rate of a link for one week. Congestion loss rate has a positive correlation with the outgoing traffic rate. Unlike congestion, corruption loss rate does not change as the link's incoming traffic rate changes. To depict the lack of correlation in all links, we compute the Pearson correlation between utilization of a link and the logarithm of its loss rates. Figure 3b shows the CDF of Pearson correlation across all links. The mean correlation between incoming link utilization and corruption loss rate is only 0.19, and 85% of the links have a correlation between -0.5 and +0.5. Hence, for most links, there is no correlation between their utilization and corruption loss rate. In contrast, the mean correlation between outgoing link utilization and corruption loss rate is 0.62, which indicates a strong positive correlation. This behavior is expected because more traffic leads to a higher congestion loss rate.

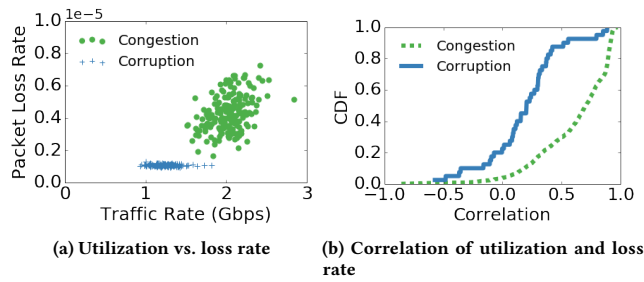


Figure 3: Corruption loss rate is less correlated with utilization than is congestion loss rate. 3a shows a scatter plot of utilization versus loss rates of a link for one week. Unlike congestion, the corruption loss rate does not change as the link’s utilization changes. 3b plots the CDF of Pearson correlation between utilization and logarithm of loss rate. The average Pearson correlation between utilization and congestion loss rate is 0.62. The average Pearson correlation between utilization and corruption loss rate is 0.19.

Because the corruption loss rate is uncorrelated with utilization, application or transport layer reactions will not resolve it. Thus, unlike congestion, packet corruption is a pernicious fault that is not mitigated when senders slowdown. Instead, it persists—to stop it, we must disable the link and then have technicians fix it. A related, unfortunate aspect of corruption losses is that they lead loss-sensitive transport protocols such as TCP to unnecessarily slow down, which does nothing to resolve corruption but does hurt application performance.

Corruption has weak spatial locality. We investigated if corrupting links tend to be spatially correlated (e.g., on the same switch or topologically close) or scattered across the DCN (uniformly and) randomly, and we found weak spatial locality. To demonstrate this finding, we first compute the fraction of switches in the DCN that have at least one link with a high corruption loss rate, i.e., in the set of the worst 10% of corrupting links. We then simulate a hypothetical setting in which the same number of corrupting links are randomly spread through the network, and again compute the fraction of switches to which they belong. We then calculate the ratio of the two switch fractions. For example, let’s say $x\%$ of switches contain the worst 10% of corrupting links. If those corrupting links are uniformly distributed, $y\%$ of switches will contain them. Then the ratio is $\frac{x}{y}$. If the ratio is 1, it suggests that corrupting links are scattered randomly across the switches. Lower ratios indicate more co-location with switches.

We repeat this analysis for 100 different values, between 0 and 100%, for the set of corrupting links chosen, and we also repeat the analysis for congested links. As Figure 4 shows, for congestion, the number of affected switch is only 20% of what the random distribution suggests. This means congested links exhibit a high degree of spatial locality. For corruption, this ratio is around 80%, which indicates weak spatial locality. We can also see that when we focus on the worst corrupting links (e.g., the top 10%), the locality

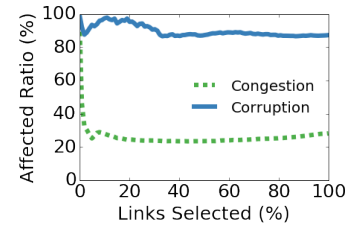


Figure 4: Links with packet corruption have weak locality.

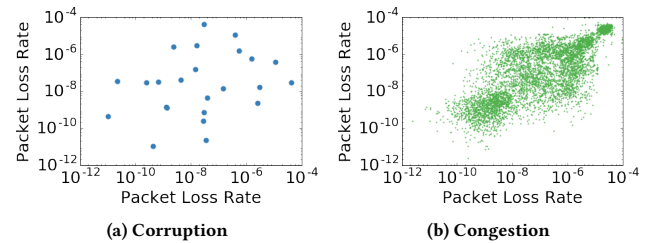


Figure 5: Corruption is highly asymmetric. 5a shows corruption loss rate at x-axis and the corruption loss rate on the opposite direction at y-axis. 5b is a similar figure for congestion loss rate.

is weaker. Thus, the worst offenders are more likely to be randomly spread in the network.

While we expected congestion to exhibit locality, the locality (albeit weak) of corruption surprised us. As we show in §4, it occurs because of shared root causes (e.g., bad switch backplane or poorly-routed fiber bundle). We also found that spatially related links start corrupting packets roughly the same time and have similar corruption loss rates. We omit these results from the paper.

Corruption is asymmetric. Corruption in one direction of the link does not imply corruption in the reverse direction. With a week’s worth of data, we observed that only 8.2% of the links among links with packet corruption had bidirectional corruption.³ For congestion, 72.7% of links among links with congestion losses had bidirectional losses. For those links with bidirectional losses, Figure 5 shows average packet loss rate on both directions of the link. For congestion, however, we see a cluster of links for which the congestion loss rates in both directions are similar and large. We speculate that high, bidirectional congestion is caused by link failures that temporarily reduce network capacity for both upstream and downstream traffic.

Corruption is uncorrelated with link location. Corruption happens at every stage of the DCN topology. We computed the probability that a link is corrupting for each stage of the network (e.g., ToR-to-aggregation, aggregation-to-ToR, aggregation-to-spine), and we did not observe any bias. This observation also implies that corruption

³This asymmetry implies that a more efficient way (in terms of network capacity) to mitigate corruption would be to disable only one direction of the link, but since current hardware and software does not allow unidirectional links, we disable both directions in CorrOpt.

does not depend on cable length, since cable lengths at higher stages tend to be longer, or the type of switch. In contrast, we find that certain stages of the DCN have significantly fewer congestion losses than the rest. We find this reduction in congestion losses to be correlated with the use of deep buffer switches. Shallow buffer switches in such stages still experience congestion losses.

4 ROOT CAUSES OF CORRUPTION

To successfully repair a corrupting link, operators need to address the root cause of corruption. We analyzed over 300 trouble tickets while monitoring all links' optical receive power (RxPower) and transmit power (TxPower), as well as their corruption statistics.⁴ This tandem monitoring of tickets and link statistics turns up a set of symptoms that are the most common signature of each root cause. In §5.2 we use these symptoms to recommend repair actions to on-site technicians to help them eliminate corruption faster.

Root cause 1: Connector contamination. An optical link consists of fiber optics cable and a transceiver on each end. Transceivers convert the signal between electrical and optical domains, and the fiber carries the optical signal. In fiber optics, the tolerance of dirt or contamination on a connector is near zero [22]. Airborne dirt particles may even scratch the connectors permanently if not removed. Fiber tips or connectors can become contaminated during installation or maintenance. Patch panels can become contaminated if they are left open to the air or scrape off foreign particles under repeated usage. Figure 6a shows an MTP fiber connection with 12 fiber cores. Prior to installation, technicians should inspect each fiber core manually using a fiber microscope. Figure 6b shows a magnified image of two cores we inspected using a P5000i Fiber Microscope [21]. In this case, the device found more than five defects larger than $2\ \mu\text{m}$ in diameter on the right-hand side fiber core and failed the test on it. Common types of contamination and defects include dirt, oil, pits, chips, and scratches [13]. Fiber cleaning can remove dirt and contamination on the connector.

Contamination reduces RxPower which increases the probability of packet corruption by making it more likely that the transceiver is unable to decode the signal correctly [38]. Since fiber optics cables and connectors are unidirectional, we find that the most probable indicator of contamination is high TxPower on both sides of the link, with low RxPower along only one direction of the link (i.e., the receiving side of corruption). As Figure 7 shows, the packet corruption of a link jumps at the same time as its RxPower drops, but the TxPower on the opposite side remains stable. In this case, cleaning the both sides of the link mitigates the corruption.

Not all forms of contamination cause low RxPower; some cause back reflections, where the RxPower remains high but the reflections interfere with signal decoding. Transceivers do not report on reflections, and thus we are not able to correctly identify this root cause all the time. Such limitations of accurate identification exist for other root causes as well, which is why the accuracy of our repair recommendations is not 100%.

Root cause 2: Damaged or bent fiber. Cable management is a tedious task in large fiber plants. A bent or damaged fiber causes the optical signal to leak out of the fiber, reducing the signal strength

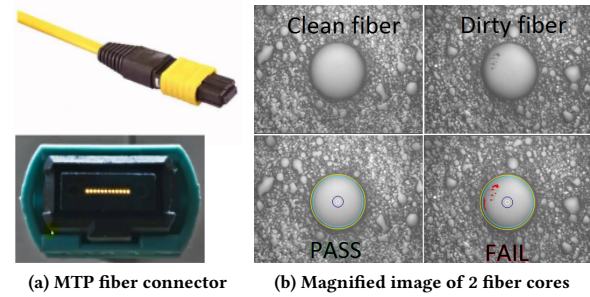


Figure 6: Dirty connection creates corruption. 6a shows an MTP fiber connection consisting of 12 fiber cores. 6b shows a magnified image of two cores. These images were taken using a P5000i Fiber Microscope to inspect and certify fiber end face quality in production data centers [21]. In this case, the tool found more than five defects larger than $2\ \mu\text{m}$ in diameter on the right-hand side fiber core. Technicians are supposed to inspect each fiber core manually prior to installation—a task that is largely ignored because it is manual and cumbersome. Similar observations are reported for other fiber types [14].

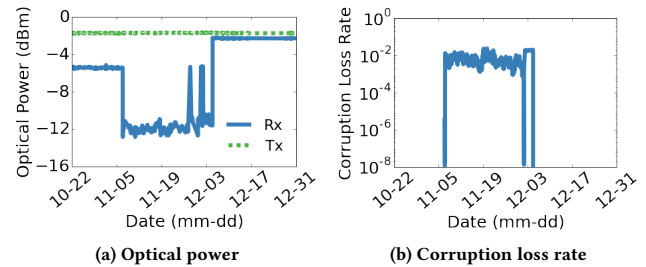


Figure 7: An example of a dirty connection causing packet corruption. RxPower suddenly drops on November 5, causing corruption loss to increase to 10^{-2} (1%). TxPower on the transmit side shows no changes. Fiber cleaning takes place on November 27 which restores RxPower level and eliminates the corruption.

in the fiber. Cables should be laid such that they are not bent beyond their specification, especially for fibers at the bottom layer of a fiber housing mount. Figure 8 shows a case in our data center; the fibers at the bottom row are too bent, causing corruption.

When we study the RxPower of damaged or bent cables, we find both sides of the link are likely to have low RxPower coupled with high TxPower. Figure 9 shows an example of a damaged fiber causing packet corruption. Another indicator of cable damage is that switches on both sides experience packet corruption, which is otherwise rare (§3).

Root cause 3: Decaying transmitters. Transceivers are built using semiconductor laser technology, and their lasers tend to have a

⁴In modern DCNs, all inter-switch links tend to be optical.

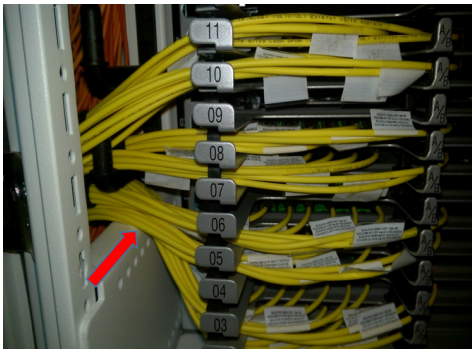


Figure 8: Bent fiber (red arrow) can cause packet corruption when the fiber cable is bent tighter than its maximum bend tolerance. When operating a large fiber plant, this situation becomes likely especially for long cables.

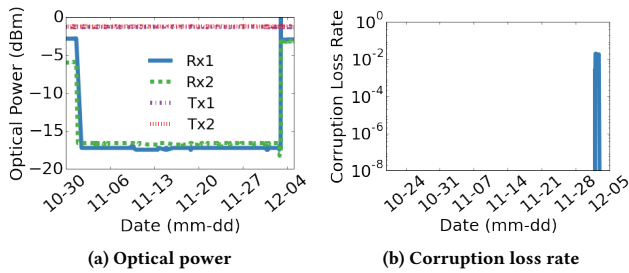


Figure 9: An example of a damaged fiber causing packet corruption. Fiber damage happens on October 30 causing both sides’ RxPower to suddenly drop at the same time. TxPower on both sides are not affected. When traffic is put on the link at the beginning of December, the corruption loss rate is around 1%. Fiber replacement restores both sides’ RxPower back to normal level.

long life expectancy, but old lasers can suffer deterioration in TxPower, leading to low RxPower and corruption on the receive side of the link. Replacing the dying transceiver can resolve the problem. The most probable symptom of decaying transmitters is that the TxPower on the send side of the link and RxPower on the receive side of the link are both low or are gradually decreasing.

Root cause 4: Bad or loose transceivers. Bad transceivers or loosely-seated ones (i.e., not properly plugged in) also cause corruption. When this happens, technicians should take out the transceiver and plug it back in (a.k.a., reseating the transceiver). If the issue is not resolved, the transceiver is likely bad and needs to be replaced.

When bad or loosely-seated transceivers cause corruption, optical TxPower and RxPower on both sides of the link are most likely high, but the link still corrupts packets. This symptom is shared by root cause 5 as well, but a distinguishing characteristic of this root cause is that only one of the links on the switch is bad. It is uncommon (but still possible) that multiple transceivers on the same switch are bad or loose.

Root cause	Most likely symptom $TxPower \rightarrow RxPower$ $RxPower \leftarrow TxPower$	Contribution
Connector contamination	$H \rightarrow H$ $L \leftarrow H$	17-57%
Bent or damaged fiber	$H \rightarrow L$ $L \leftarrow H$	14-48%
Decaying transmitter	$* \rightarrow *$ $L \leftarrow L$	< 1%
Bad or loose transceiver	$H \rightarrow H$ $H \leftarrow H$ (single link)	6-45%
Shared component failure	$H \rightarrow H$ $H \leftarrow H$ (co-located links)	10-26%

Table 2: Summary of root causes of corruption, their symptoms and their relative contribution in our data centers.

Root cause 5: Shared-component failure. Some infrastructure components in a DCN, such as breakout cables⁵ and switches, are shared by multiple links. A faulty breakout cable causes four links on the same switch to have packet corruption at the same time. Breakout cable replacement can resolve the issue. Faults in the switch backplane can also cause multiple links to experience corruption. In such cases, several links on the shared infrastructure suffer packet corruption, despite good optical power levels on all of them. In addition, the corruption loss rate on these links is similar. When switches have unused ports that are not affected by the failure, rewiring can resolve the issue. Otherwise, the switch has to be replaced. This root cause is primarily responsible for the spatial locality of packet corruption (§3). We find in our data that links experiencing packet corruption because of other root causes, which usually accompany low RxPower, exhibit no locality.

Table 2 summarizes the root causes mentioned above, their symptoms and their relative contribution in our data centers. We use the notation of $TxPower \rightarrow RxPower$ to indicate the power levels of each side of optical links. H and L indicate if the power level is above or below the acceptable threshold (determined by the transceiver technology and loss budget of links). The percentage of contribution of each root cause is presented as a range because our ticket diaries show that technicians often take multiple actions (e.g., clear the connectors and reseal the transceiver) without logging which action resulted in the repair. When a root cause is present in such a bundle, we assume that it was not the culprit to compute the low end of the reported range and we assume that it was the culprit to compute the high end of the reported range.

5 MITIGATING CORRUPTION

There are two aspects to CorrOpt, our system to mitigate corruption. First, to protect applications from corruption, we disable corrupting links, while meeting configured capacity constraints. Meeting capacity constraints is important because otherwise we may trade

⁵ A breakout cable splits a high-speed port (e.g, 40Gbps, 100Gbps) into several low-speed ports (e.g, 10Gbps, 25Gbps). It is typically used between switches with different port speed.

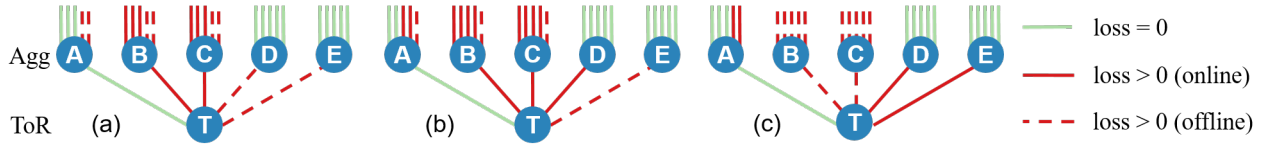


Figure 10: Example of problems with switch-local checking, with ToR capacity constraints of $c=60\%$. (a): Every switch keeps $s_c=c=60\%$ of its uplinks alive, resulting in 8 disabled links, but only 9 out of 25 paths to the spine are still available for T, far below the constraint of 60%. (b): When $s_c=\sqrt{c} = 0.77$ of the links are kept online, the ToR capacity constraint is met, but only 4 links can be disabled. (c): The optimal solution, which has 12 disabled links offline and meets the capacity constraints.

off corruption losses for heavy congestion losses. For practical reasons, we only consider disabling links as a strategy in this paper; it requires minimal changes to our existing infrastructure. We will consider other strategies, such as error coding, source routing, or traffic engineering to move sensitive traffic away from corrupting links, in future work. That said, any such strategy would still need to disable corrupting links at some point to enable operators to fix them. Our strategy to detect and disable corrupting links can be used in combination with these strategies.

If we rely solely on disabling links for corruption mitigation, the DCN will have fewer and fewer links as time progresses. Instead, we must also fix the root cause of corruption, so links can be enabled again. Thus, the second aspect of CorrOpt is generating repair recommendations for disabled links based on root causes and symptoms described in §4. Our recommendations reduce both repair time and packet loss (§7.2).

5.1 Disabling Corrupting Links

While disabling corrupting links reduces corruption losses, it also reduces network capacity. In the extreme cases, especially because of the locality of corrupting links, blindly disabling links can create hotspots, and, hence, engender heavy congestion losses; it may even partition the network.

To lower corruption losses without creating heavy congestion, we consider a common capacity metric [24, 29, 34]: the fraction of available valley-free paths from a top-of-rack switch (ToR) to the highest stage of the network (i.e., the spine). This metric quantifies available capacity and redundancy for a ToR after links are disabled. Because traffic demand can differ across ToRs [17], we allow per-ToR thresholds. Our data show up to 15% of corrupting links cannot be disabled due to capacity constraints under realistic configurations (e.g., when every ToR has threshold between 50–75%).

CorrOpt determines the subset of links to disable based on the impact of corrupting links that remain active. Each link l with packet corruption rate of f_l has impact $I(f_l)$, where $I(\cdot)$ is a monotonically increasing penalty function that reflects the relationship between application performance and loss rate [27, 36]. CorrOpt aims to minimize the total penalty of packet corruption, i.e., $\sum_{l \in \text{links}} (1 - d_l) \times I(f_l)$, where d_l is 1 if the link is disabled and 0 otherwise. Our goal is to determine the value of d_l for each link l , while meeting capacity constraints.

However, as we prove in Appendix A (via reduction to 3-SAT) this problem is computationally difficult.⁶

THEOREM 5.1. *Deciding which links to disable in a Clos topology, s.t. the total penalty of packet corruption is minimized under capacity constraints, is NP-complete.*

Because of the complexity, we cannot quickly determine the optimal set of links to disable. Speed is desirable to protect applications from corruption, but it is not possible to be both fast and optimal.

State-of-the-art: switch-local checking. Current DCN operators opt for speed [26]. When a new corrupting link is found, a controller decides whether it can be disabled based on the number of available uplinks at the switch to which it is attached. For a threshold of s_c and a switch with m uplinks, $\lfloor m \times (1 - s_c) \rfloor$ of the uplinks can be disabled. For example, with $m = 5$ uplinks and $s_c = 60\%$, at most two uplinks can be disabled. When a link is enabled, after repairing corruption or other problems, the same check is run for all active corrupting links to see if additional links, which could not be disabled before, can be disabled now.

Unfortunately, switch-local checks are highly sub-optimal. Figure 10 shows an example, where T is a ToR with five uplinks, to switches (A through E) that also have five uplinks each. Corrupting links are in red, and dashed lines represent disabled links. Suppose we want to enforce a per-ToR capacity constraint of $c=60\%$. If we directly map c to the switch-local constraint, i.e., $s_c=c$, Figure 10(a) shows the network state that will emerge. The direct mapping leads to disabling eight corrupting links. However, ToR T now has only nine of 25 (36%) possible paths to the spine, far below the desired limit of 60%.

This problem can be fixed by enforcing a switch-local capacity constraint of $s_c = \sqrt{c} = 0.77$ because this forces c fraction of paths to the core switches to be available. But now, as shown in Figure 10(b), each switch can disable only one corrupting uplink, for a total of four disabled links (out of a total of 16 corrupting links). The optimal solution, however, shown in Figure 10(c), can disable as many as 12 corrupting links, for a much lower total penalty due to active corrupting links.

Generalizing the example above, in a simple ToR-aggregation-spine-topology, a capacity constraint of c requires every switch to keep \sqrt{c} of its uplinks. Otherwise, the capacity constraint can be violated. The gap widens when the DCN has more tiers: with r tiers above the ToR-level, a switch-local algorithm needs to keep $\sqrt[r]{c}$ fraction of uplinks active.

⁶The NP-hard problem stated in [9] is orthogonal to our formulation, as it moves logical machines between physical machines.

Another limitation of a switch-local checker is that it cannot handle different ToR requirements well. If one ToR has a high capacity requirement c' , all upstream switches need to keep $\sqrt{c'}$ uplinks active. A switch-local checker may not be able to disable a single link in extreme cases.

CorrOpt's approach. CorrOpt achieves both speed and optimality using a two-pronged approach. First, when a new corrupting link is found, it runs a *fast checker* for a quick response that exploits global network state to bypass the sub-optimality of switch-local checking. Second, when links become active, CorrOpt runs an *optimizer* that globally optimizes over all active corrupting links in the network. Link activations allow other remaining corrupting links to be turned off. Those links tend to have lower loss rates than newly arrived corrupting link due to the fast checker disabling lossy links, which gives us time to solve a hard problem. By analyzing the failure structures in our data set, we are able to efficiently solve the practical instances of this NP-complete problem. We now provide more detail on the two components.

Fast checker. Conceptually, when a new corrupting link l arrives, CorrOpt counts the remaining paths for each ToR to the spine assuming l is removed from the topology. If no ToR's constraint is violated, CorrOpt disables l and creates a maintenance ticket for it with a recommended repair. This process is repeated for each new corrupting link. As long as no link is activated since its last run, the network state after the fast checker runs is maximal, i.e., no more links can be disabled. If no link was activated since the last run of the fast checker, the optimizer must have left the network in a maximal state. Thus, we never need to run fast checker on old corrupting links that could not be disabled earlier.

Because of its exact counting of paths, our fast checker can disable more links than switch-local checking. A naive implementation of the fast checker is to iterate over all the path from ToR switches to the spine switches in order to count the number of available paths for each ToR. The naive implementation is slow because a large data center network can possibly have over millions of paths. Using information about all links E in the DCN, we efficiently implement CorrOpt's fast checker as follows. First, for each switch v_2 in the second-highest stage, we count the active (one-hop) paths $p_1(v_2)$ to the spine (i.e., the highest stage). Then, each switch v_3 in the third-highest stage adds $p_1(v_2)$ to each of its active uplinks, obtaining the number of two-hop paths $p_2(v_3)$ to the spine. This process is iterated until the ToR-stage is reached.

With this information, to see if l can be safely disabled, we check the downstream of l , updating the path counts with the same method, beginning with the switch directly downstream of l . If all downstream ToRs of l meet the capacity constraints with l offline, l is disabled. Conceptually, we perform $O(1)$ operations per link, resulting in a linear runtime of $O(|E|)$. In our experiments, the fast checker takes only 100-300 ms for the largest DCN, effectively providing instantaneous decisions.

Optimizer. When a link is enabled, one option is to rerun the fast checker on all active corrupting links, as is done today in switch-local checks. However, we can now afford to run a potentially-slower computation to determine the optimal subset of links to

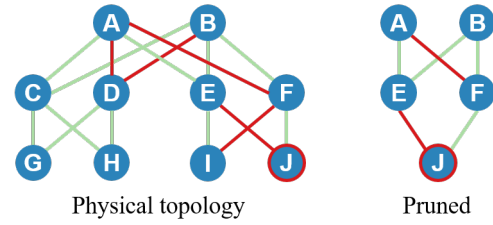


Figure 11: Example of topology pruning. If capacity constraint is 50%, only ToR J will violate the constraint if all corrupting links (in red) are disabled. Hence, we only need to consider the pruned topology and can safely disable the other three links.

disable. The optimization problem is what we defined earlier, operating over the set of active corrupting links.⁷

Even though the problem is NP-complete, we can provide a fast exact algorithm in practice. First, we find that, under realistic capacity constraints, 99% of the ToRs can be ignored because their capacity constraints will not be violated even if all corrupting links are disabled. Only the links that are in danger of capacity constraint violation need to be considered. To identify such links, we run fast checker's path counting procedure on the network with all corrupting links considered disabled, identifying all ToRs V whose capacity constraints are violated. Only disabling links upstream of the ToRs in V can violate capacity constraints. All corrupting links not upstream of V can hence be safely disabled, thus pruning the topology.

For instance, in Figure 11, assume the capacity constraint is 50%. The corrupting links are shown in red, and if we were to disable all of them, ToRs G, H, and I will have at least two out of four paths to the spines, but ToR J will have only one. Thus, we can remove all links and switches except those upstream of J, and the three removed corrupting links can be safely disabled.

Next, we need to decide which remaining corrupting links in the pruned topology can be disabled. CorrOpt iterates through all possible subset to measure (1) whether the capacity constraint is met if the entire subset is turned off (2) the total penalty if the subset is turned off. To speed up, CorrOpt uses a "reject cache" to memorize subsets that can fail capacity constraint. When CorrOpt iterates through a subset that is a super set of any set in the cache, the subset is immediately ignored. For example, in Figure 11, $\{AF, E\}$ can be kept in the cache. Any subset S such that S is a superset of $\{AF, E\}$ is guaranteed to fail the capacity constraint and thus can be ignored.

The output of CorrOpt's optimizer is an exact solution to the optimization problem. Pruning only removes links that can be safely disabled and the "reject cache" only skips infeasible link sets. In our experiments, the combination of both techniques allows us to finish

⁷For practical reasons, CorrOpt does not enable corrupting links before they have been repaired. In theory, we can further reduce corruption losses by doing so; e.g., pre-maturely enabling a link with a lower corruption rate may allow a link with a higher corruption rate to be disabled. On our small to medium DCNs, the performance of this optimal version was close to that of CorrOpt. We could not evaluate this version on our large DCNs because of its computational complexity, which is worse than CorrOpt's optimizer since it considers a bigger set of links at each step.

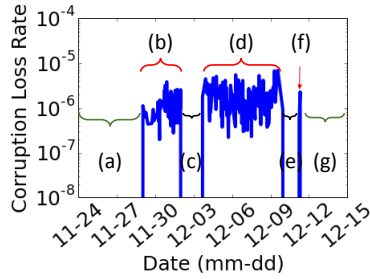


Figure 12: An example of unsuccessful repair actions on a link. (a) A healthy state with corruption loss rate below 10^{-8} . (b) Starts corrupting packets. (c) Disabled for repair. (d) Enabled after the repair but starts corrupting packets again. (e) Disabled again. (f) Enabled after but the repair failed again. (g) Disabled again for repair, and the repair is finally successful.

optimizer runs in less than one minute on a 1.3 GHz computer with 2 cores.

5.2 Corruption Repair

Simply stated, repairing corruption in today’s DCNs is cumbersome. Unlike switch configuration errors or congestion, corruption cannot be remedied via a software-based reaction. For example, as mentioned in §4, dirt on connectors can cause corruption, and the only repair is to manually clean the connections. If the root cause of the corruption is not correctly diagnosed, on-site technicians must rely on guesswork when deciding what action to take.

Network technicians currently use manual diagnosis. When assigned to a ticket, they manually inspect the transceiver and the fiber to find tight bends or damage. If equipment is not connected firmly, they reconnect it. If tight bends or damage are found on the fiber, the technicians replace the fiber. If they cannot find any problem visually, they may choose to clean the connector with an optical cleaning kit [30].

If the repair does not address the actual cause of packet corruption, the link will continue to corrupt packets as soon as the link is enabled. Figures 7 and 9 show examples of successful repair. In contrast, Figure 12 shows a series of two unsuccessful repair attempts. Both include cleaning the fiber and reseating the transceiver. Finally, on the third try, the technician replaces the fiber and fixes the corruption.

This whole process takes several days. In between repair attempts, the link is enabled and a new ticket is generated when it is disabled again. Generated tickets are placed in a FIFO queue; thus, the exact time needed for a fix depends on the number of tickets in the queue. Our analysis of 3400 tickets shows that, on average, it takes two days for technicians to resolve a ticket; this means, each failed repair attempt adds two more days during which the link must be disabled.

Unsuccessful repairs also increase the likelihood of collateral damage because technicians need to enter the facility more often. Each entry poses a risk of them affecting something unrelated (e.g.,

Algorithm 1 CorrOpt’s recommendation engine

```

1: function RECOMMEND REPAIR(link)
2:   neighbors  $\leftarrow$  links sharing same component (i.e., switch)
3:   if has_corruption(neighbors) then
4:     return Replace shared component
5:   if has_corruption(opposite_side) then
6:     return Replace cable/fiber
7:   Rx1  $\leftarrow$  RxPower of link
8:   Rx2  $\leftarrow$  RxPower of opposite side of link
9:   Tx2  $\leftarrow$  TxPower of opposite side of link
10:  if Tx2  $\leq$  PowerThreshTx then
11:    return Replace transceiver on the opposite side
12:  if Rx1  $<$  PowerThreshRx and Rx2  $<$  PowerThreshRx then
13:    return Replace cable/fiber
14:  if Rx1  $<$  PowerThreshRx then
15:    return Clean fiber
16:  else
17:    if Transceiver is not reseated recently then
18:      return Reseat transceiver
19:    else
20:      return Replace transceiver

```

tripping over cables, replacing the wrong cable or transceiver, or accidentally powering off equipment).

In CorrOpt, we seek to improve the accuracy of repair by leveraging our observations of the most likely symptoms of corruption root causes (§4) in terms of optical power levels and the link’s history. Our strategy is listed in Algorithm 1. It first uses packet corruption rate on neighboring links to identify shared component failures. Then it uses TxPower on the opposite side to detect decaying transmitters. CorrOpt uses RxPower to separate optical and non-optical issues. With non-optical issues, the only solution is to try reseating the transceiver, and then to replace it.

CorrOpt uses $Power_{ThreshRx}$ ($Power_{ThreshTx}$) per optical technology as the minimal RxPower (TxPower) threshold. When both ends of a link have RxPower below $Power_{ThreshRx}$, this suggests bent or damaged fiber. Connector contamination tends to cause RxPower to be low in one direction. Cleaning connectors with fiber cleaning kits can often fix corruption.

CorrOpt’s recommendation engine has been deployed in our DCNs since October 2016. §7.2 evaluates its effectiveness. In our experience, machine learning techniques can produce similar repair accuracy. We choose our approach because it is more intuitive.

6 IMPLEMENTATION

Figure 13 shows the workflow and system components of CorrOpt. When a switch detects packet corruption, it reports to the CorrOpt controller. The controller uses the fast checker logic to quickly determine if the link can be safely disabled. If the link is disabled, the recommendation engine (§5.2) generates a ticket with a suggested repair procedure, based off the monitoring data (collected by another system). When a link is activated, CorrOpt uses the optimizer logic to check if any active corrupting links can be disabled.

We prototyped fast checker and optimizer with around 500 lines of python code. We integrated CorrOpt’s recommendation engine into the cloud provider’s infrastructure with around 50 lines of C# code.

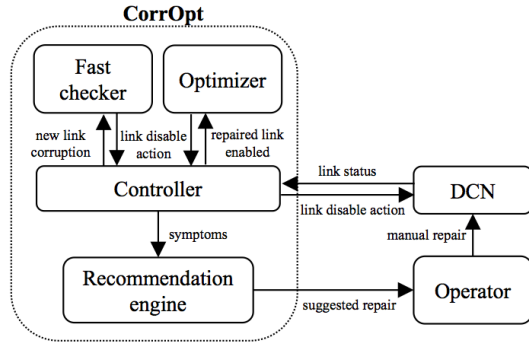


Figure 13: CorrOpt's system components and workflow.

7 EVALUATION

We now evaluate CorrOpt for *i*) its ability to protect applications by safely disabling corrupting links, while meeting capacity constraints; and *ii*) its ability to speed repairs by correctly identifying the root cause. The first evaluation uses simulations based on data from our DCNs, and the second uses our deployment of CorrOpt's repair recommendation engine for three months. We study these two factors individually in §7.1 and §7.2, and we quantify their combined impact in §7.3.

7.1 Disabling Links

We simulate the impact of CorrOpt using the topologies and link corruption traces from two production DCNs, a large DCN with $O(35K)$ links and a medium-sized DCN with $O(15K)$ links. The trace period is from Oct to Dec 2016.

We quantify the effectiveness of CorrOpt at disabling links using "total penalty." Each corrupting link l with corruption rate f_l incurs a penalty of $I(f_l)$ per second (§5), and the total penalty per second is $\sum_{l \in \text{links}} (1 - d_l) \times I(f_l)$, where d_l is 1 if the link is disabled and 0 otherwise. For simplicity, results in this paper use $I(f_l) = f_l$. Thus, the total penalty is proportional to corruption losses (assuming equal utilization on all links).

We compare CorrOpt with "switch-local," the link disabling technique used today. As we discussed earlier, for this method to guarantee a capacity constraint of c , it should be configured with $s_c = \sqrt{c}$ for three-stage DCNs (which is what we study).

To isolate the impact of link disabling strategy, we couple both methods with the same repair effectiveness (as CorrOpt's). When a link is disabled, it is put into a queue of links that are waiting to be fixed. Links stay in that queue for two days, the average service time in our DCNs (§5.2). Based on our observed repair accuracy (§7.2), 80% of the links are repaired correctly after this time. The remaining take two rounds of fix, so the overall it takes them four days to be enabled again.

Figure 14 shows the performance of both methods for the two DCNs, when the capacity constraint is $c=75\%$ for every ToR. The x -axis is time, and the y -axis is total penalty per second. We see that the penalty of the switch-local checker is much higher, because of its sub-optimality that we illustrated earlier. It is flat for switch-local approach because there is a set of corrupting links switch-level

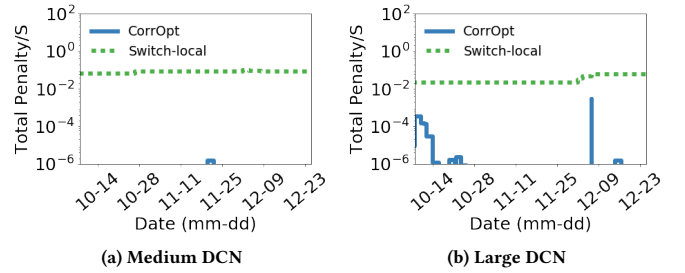


Figure 14: Total penalty per second of switch-local and CorrOpt when the capacity constraint is 75% for every ToR.

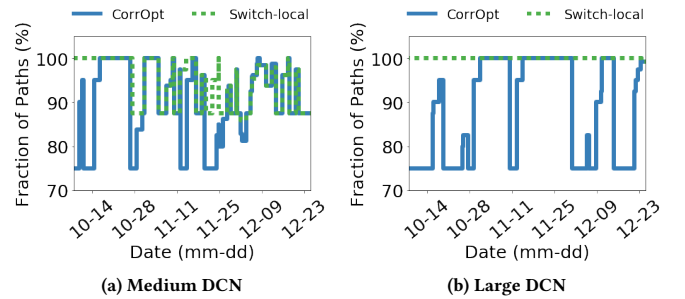


Figure 15: Fraction of available paths to the spine for the worst ToRs when the capacity constraint is 75%.

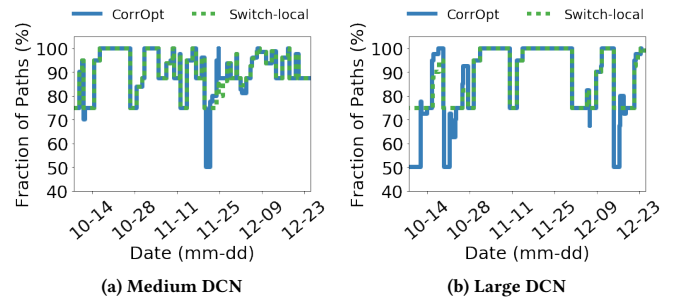


Figure 16: Fraction of available paths to the spine for the worst ToRs when the capacity constraint is 50%.

approach is not able to disable and in our model, they corrupt packets at constant rates. In contrast, CorrOpt can disable the vast majority of the corrupting links, leading to a much lower penalty. The penalty varies with time based on the number and relative locations of corrupting links in the data.

The inability of the switch-local checker to disable links is visible in Figures 15 and 16, which show the worst ToR's fraction of available paths to the spine when the capacity constraint is 75% and 50%. When lines overlap, it means for some period of time, performance of CorrOpt is the same of switch-local check. Overall, we see that CorrOpt can hit the capacity limit as needed, but

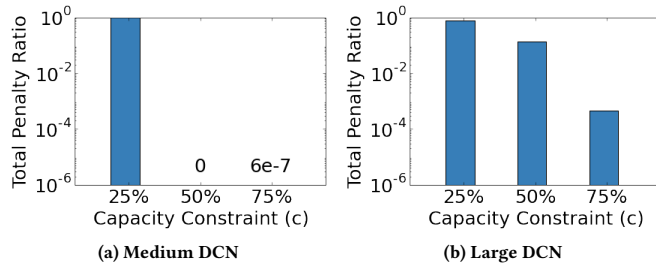


Figure 17: Total penalty of CorrOpt divided by switch-local for different capacity constraints.

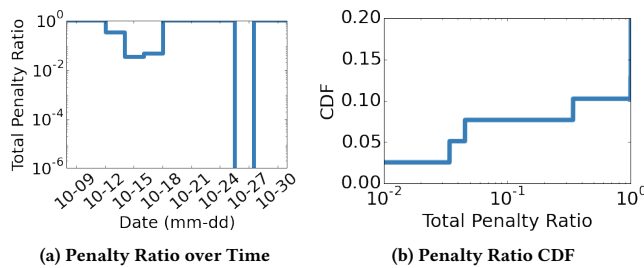


Figure 18: Gain of optimizer over using fast checker alone in the large DCN. (a) The ratio of total penalty of CorrOpt (fast checker + optimizer) divided by using fast checker alone. (b) The CDF of this ratio over the entire simulation period.

switch-local does not disable enough links even though it is not limited by the capacity constraint.

Impact of the capacity constraint. The advantage of CorrOpt over today’s switch-local checks depends on the capacity constraint. If the constraint is lax, both methods are expected to perform similarly, as both can turn off almost all corrupting links. However, when the constraint is more demanding, the intelligent decision making of CorrOpt begins to shine. For different capacity constraints, Figure 17 shows the total penalty, integrated over time, of CorrOpt divided by that of the switch-local checker. Since our penalty function is linear in corruption losses, this ratio represents the reduction in the amount of corruption losses.

We see that when the capacity constraint is lax ($c=25\%$), as expected, there is no difference between the two methods. However, when the capacity constraint is 50% or higher, a more realistic regime, CorrOpt outperforms the switch-local checker. On the medium size data center, with a capacity constraint of 50%, CorrOpt can eliminate almost all corruption while the switch-local check keeps some corrupting links active. Thus, the total penalty ratio drops to 0. When the capacity constraint is 75%, CorrOpt’s total penalty is three to six orders of magnitude lower.

Fast checker vs. optimizer. To isolate the performance gain of fast checker and optimizer, we simulate the large DCN using fast checker alone, which is run both when new corrupting links appear and disabled links are activated. We bin time into one-hour chunks

and estimate the total penalty incurred using fast checker alone and with the full CorrOpt logic. Figure 18a shows the total penalty ratio of using CorrOpt versus using fast checker only for a month-long period. We see most of the time, optimizer does not reduce penalty. However, during certain periods, it can significantly reduce corruption losses compared to using fast checker alone. Figure 18b shows CDF of the average ratio of penalty of CorrOpt over that with using fast checker alone. Optimizer does not lower the ratio for 90% of the time. For 7% of the time, optimizer can reduce the total penalty per second by at least one order of magnitude.

7.2 Accuracy of Repair Recommendations

CorrOpt’s repair recommendation engine has been deployed across 70 DCNs of different sizes since Oct 2016. Because of certain limitations of the current infrastructure, the deployed version is simpler than the version outlined in §5.2. It uses a single RxPower threshold rather than customizing it to the links’ optical technology (information about which was not readily available), and it does not consider historical repairs or space locality. As a result of these simplifications, the results below underestimate the efficacy of our repair recommendations.

To evaluate CorrOpt, we analyze tickets generated between Oct 22 and Dec 31 2016. In this period, it generated close to two thousand tickets with a repair recommendation. Not all generated tickets have a repair recommendation because we cannot get optical power information from all types of switches. We deem repair successful if we do not see another ticket for the same link within a week. Because corruption faults are infrequent, if a link experiences corruption soon after a repaired, it is likely that the repair was not successful.

Based on this analysis, the success rate of repair was 58.0%, which is much lower than our expectation. To investigate, we read diaries of 322 tickets. We found that 30% of the time, technicians were ignoring the recommendations! Since CorrOpt is newly-deployed, not all operators have been informed or trained to leverage the information it provides.

When the technicians followed our recommendation, the success rate was 80%. In contrast, our analysis of tickets before CorrOpt’s deployment revealed that the previous repair success rate was 50%. The higher success rate of CorrOpt implies the links can be put back into service sooner; at the same time, it reduces the risk of collateral damage that occurs with each manual intervention.

CorrOpt’s higher accuracy of repair also lowers corruption losses because that leads to more healthy links in the DCN, which allows more corrupting links to be disabled while meeting capacity constraints. To quantify this effect, we ran simulations similar to those in the previous section and considered two different repair processes. With CorrOpt, 80% the links are repaired in two days and the rest in four days (i.e., requiring two attempts). Without CorrOpt, 50% of the links are repaired in two days and the rest in four days. In both cases, CorrOpt’s algorithm was used to disable links.

Figure 19 shows the results for different capacity constraint for both medium and large DCNs. The penalty is normalized to that of the setting without CorrOpt. We see that, in addition to their other benefits, CorrOpt repair recommendations reduce corruption losses by 30% when the capacity constraint is 75%.

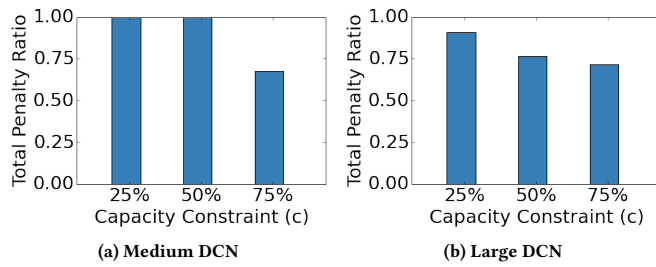


Figure 19: CorrOpt’s repair recommendations also help lower corruption loss. The graph plots the ratio of total penalty with and without CorrOpt’s recommendation engine.

7.3 Combined Impact

We conclude by evaluating the combined impact of CorrOpt’s strategy of disabling links and repair recommendations. (Previous sections studied their impact individually.) We compare it to the current practice of using switch-local checks to disable links and 50% repair accuracy.

In terms of reducing packet losses, the results are similar to those in Figure 17. That is because most of the gain stem from its strategy for disabling links, though its higher repair accuracy has other benefits noted above. Overall, in the realistic capacity constraint regime of 75%, CorrOpt reduces corruption losses by three to six orders of magnitude.

Finally, we also find that the massive reduction in corruption losses with CorrOpt does not come at the expense of significantly reduced network capacity. We measure the average fraction of paths to the spine available for each ToR when the capacity constraint is 75%. We find that, compared to the current practice, CorrOpt reduces this average by at most 0.2% across all one-second time intervals.

8 FUTURE EXTENSIONS

We discuss a few directions for extending CorrOpt.

Accounting for the impact of repair. While disabling a link has limited local effect, we found in our deployment that repairing it can sometimes cause collateral damage. For example, when one link in a breakout cable has packet corruption, to repair the breakout cable, an additional three, healthy links have to be turned off. A future extension of CorrOpt would be to account for such collateral impact, when deciding which links to disable for repair, based on a finer-grained view of the topology and its dependencies.

Removing traffic instead of disabling links Today, when CorrOpt completely disables corrupting links (when capacity constraints permit that), but based on our deployment experience, we believe that removing traffic from the link (e.g., by increasing its routing cost) is a better strategy. This way, when the link is repaired, we can run test traffic to confirm if the repair succeeded without affecting actual traffic. Further, monitoring data on optical power levels will continue to flow in (which otherwise stops when the link is disabled).

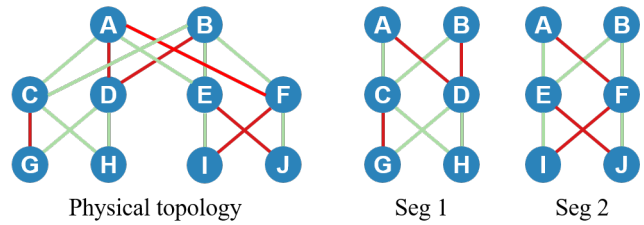


Figure 20: Example of topology segmentation. The corrupting links to D affect ToRs G,H, and the leftmost link affects G, resulting in Segment 1. The corrupting link from A to F affects ToRs I,J, with the uplinks of I,J only affecting themselves respectively, resulting in Seg 2. We can thus optimize Seg 1 and Seg 2 independently. Pruning shrinks Seg 1,2 further, depending on capacity constraints.

Speeding optimizer with topology segmentation. Our optimizer suffices for today’s DCNs, but it may need to be extended for larger DCNs or for those with more corrupting links. We can do so by dividing corrupting links into non-overlapping segments such that the decision of disabling them is independent of other segments. Figure 20 shows an example. Such segmentation significantly reduces the search space.

Load balancing. CorrOpt disables corrupting links and thus makes the network topology asymmetric. Advanced network load balancing is needed when utilization is high or a significant subset of links are off. Standard load balancing techniques [1] work seamlessly atop CorrOpt. Links taking offline by CorrOpt can be seen as link failures which is a standard input into load balancing schemes. Flows on corrupting links have to be re-routed before CorrOpt taking the links off. This can cause packet re-ordering and lower network performance temporarily. Flowlet re-routing [1] can avoid this problem.

9 RELATED WORK

Our work follows a rich body of work on understanding, diagnosing, and mitigating faults in large, complex networks. While it is not possible to cover everything here, we place our work in the context of the most relevant, recent work.

Packet corruption in DCNs. Some work has acknowledged corruption as a problem. For instance, NetPilot [34] observes that corruption hurts application performance and develops a method to locate corrupting links without access to switch counters. RAIL [38] studies the optical layer of DCNs, finding that RxPower is generally high, but instances of low RxPower can cause packet corruption. We study packet corruption in more detail, including its characteristics and root causes (we find these go beyond low RxPower).

Faults in DCNs. Many prior studies have considered other types of faults in DCNs [6, 8, 19]. For instance, Gill et al. [18] study equipment failures in DCNs, characterizing different elements’ downtime and failure numbers, combined with an impact estimation and redundancy analysis. Our focus is on a different type of fault—packet corruption—and its mitigation.

Fault mitigation. Most work on fault mitigation focuses on congestion or fail-stop faults, using techniques such as load balancing and fast rerouting [1, 7, 25, 33, 35]; however, these are less relevant for corrupting links (e.g., reducing traffic on the link will not alleviate corruption). RAIL [38] studies a setting where corruption is the norm (because optical transceivers are used in a non-conventional manner) and places only loss-tolerant traffic on corrupting links. We view corruption as an anomaly and mitigate it by disabling corrupting links, so they can be repaired. zUpdate [24] and NetPilot [34] depend on knowledge of future traffic demand to further reduce congestion loss when handling corrupting links or network update. Those techniques are complementary to CorrOpt's link disabling techniques. CorrOpt can work in data center settings where future traffic demand is not available.

Root cause diagnosis. Using optical-layer characteristics to diagnose network faults was previously proposed by Kompella et al. [23]. Ghobadi et al. [16] use optical-layer statistics to help predict failures in backbone networks. Our work uses an optical-layer monitor to help determine the root cause of packet corruption in DCNs.

10 CONCLUSION

Our analysis of packet corruption across many DCNs showed that the extent of corruption losses is significant. It also showed that, compared to congestion, corruption impacts fewer links but imposes heavier loss rates, and the corruption rate of a link is temporally stable and uncorrelated to its utilization. CorrOpt, our system to mitigate corruption, lowers corruption losses by three to six orders of magnitude by intelligently selecting which corrupting links to disable while meeting configured capacity constraints. It also generates repair recommendations that are guided by common symptoms of different root causes. This recommendation engine is deployed on all data centers of a large cloud provider, where it improved the accuracy of repair by 60%.

ACKNOWLEDGMENTS

We thank David Bragg, Jamie Gaudette and Shikhar Suri for helping us design the recommendation engine. We thank Hui Ma and Shikhar Suri for helping with the deployment of our monitoring system and the recommendation engine. We also thank our shepherd Minlan Yu and the anonymous reviewers for their helpful feedback on the paper. Klaus-Tycho Förster is supported by the Danish VILLUM FONDEN project "Reliable Computer Networks (ReNet)".

REFERENCES

- [1] Mohammad Alizadeh, Tom Edsall, Sarang Dharmapurikar, Ramanan Vaidyanathan, Kevin Chu, Andy Fingerhut, Vinh The Lam, Francis Matus, Rong Pan, Navindra Yadav, and George Varghese. 2014. CONGA: Distributed Congestion-aware Load Balancing for Datacenters. In *SIGCOMM*.
- [2] Mohammad Alizadeh, Albert Greenberg, David A. Maltz, Jitendra Padhye, Parveen Patel, Balaji Prabhakar, Sudipta Sengupta, and Murari Sridharan. 2010. Data Center TCP (DCTCP). In *SIGCOMM*.
- [3] Mohammad Alizadeh, Abdul Kabbani, Tom Edsall, Balaji Prabhakar, Amin Vahdat, and Masato Yasuda. 2012. Less is More: Trading a Little Bandwidth for Ultra-low Latency in the Data Center. In *NSDI*.
- [4] Mohammad Alizadeh, Shuang Yang, Milad Sharif, Sachin Katti, Nick McKeown, Balaji Prabhakar, and Scott Shenker. 2013. pFabric: Minimal Near-optimal Data-center Transport. In *SIGCOMM*.
- [5] Behnaz Arzani, Selim Ciraci, Boon Thau Loo, Assaf Schuster, and Geoff Outthred. 2016. Taking the Blame Game out of Data Centers Operations with NetPilot. In *SIGCOMM*.
- [6] Peter Bailis and Kyle Kingsbury. 2014. The Network is Reliable. *Commun. ACM* (2014).
- [7] Theophilus Benson, Ashok Anand, Aditya Akella, and Ming Zhang. 2011. MicroTE: Fine Grained Traffic Engineering for Data Centers. In *CoNEXT*.
- [8] Kashif Bilal, Marc Manzano, Samee U. Khan, Eusebi Calle, Keqin Li, and Albert Y. Zomaya. 2013. On the Characterization of the Structural Robustness of Data Center Networks. *IEEE Trans. Cloud Computing* (2013).
- [9] Peter Bodik, Ishai Menache, Mosharaf Chowdhury, Pradeepkumar Mani, David A. Maltz, and Ion Stoica. 2012. Surviving Failures in Bandwidth-constrained Data-centers. In *SIGCOMM*.
- [10] Neal Cardwell, Yuchung Cheng, C. Stephen Gunn, Soheil Hassas Yeganeh, and Van Jacobson. 2016. BBR: Congestion-Based Congestion Control. *ACM Queue* (2016).
- [11] J. D. Case, M. Fedor, M. L. Schoffstall, and J. Davin. 1990. Simple Network Management Protocol (SNMP). (1990).
- [12] Nandita Dukkkipati, Matt Mathis, Yuchung Cheng, and Monia Ghobadi. 2011. Proportional Rate Reduction for TCP. In *IMC*.
- [13] FiberStore. 2017. Fiber Optic Inspection Tutorial. <http://www.fs.com/fiber-optic-inspection-tutorial-aid-460.html>. (2017).
- [14] Fiber for Learning. 2017. Fiber Hygiene. <http://fiberforlearning.com/welcome/2010/09/20/connector-cleaning/>. (2017).
- [15] M. R. Garey and David S. Johnson. 1979. *Computers and Intractability: A Guide to the Theory of NP-Completeness*. W. H. Freeman.
- [16] Monia Ghobadi and Ratul Mahajan. 2016. Optical Layer Failures in a Large Backbone. In *IMC*.
- [17] Monia Ghobadi, Ratul Mahajan, Amar Phanishayee, Nikhil Devanur, Janardhan Kulkarni, Gireja Ranade, Pierre-Alexandre Blanche, Houman Rastegarfar, Madeleine Glick, and Daniel Kilper. 2016. ProjecToR: Agile Reconfigurable Data Center Interconnect. In *SIGCOMM*.
- [18] Phillipa Gill, Navendu Jain, and Nachiappan Nagappan. 2011. Understanding Network Failures in Data Centers: Measurement, Analysis, and Implications. In *SIGCOMM*.
- [19] Ramesh Govindan, Ina Minei, Mahesh Kallahalla, Bikash Koley, and Amin Vahdat. 2016. Evolve or Die: High-Availability Design Principles Drawn from Googles Network Infrastructure. In *SIGCOMM*.
- [20] Peter Hoose. 2011. Monitoring and Troubleshooting, One Engineer's rant. <https://www.nanog.org/meetings/nanog53/presentations/Monday/Hoose.pdf>. (2011).
- [21] JDSU. 2017. P5000i Fiber Microscope. <http://www.viavisolutions.com/en-us/products/p5000i-fiber-microscope>. (2017).
- [22] Edward John Forrest Jr. 2014. *How to Precision Clean All Fiber Optic Connections: A Step By Step Guide*. CreateSpace Independent Publishing Platform.
- [23] Ramana Rao Kompella, Albert Greenberg, Jennifer Rexford, Alex C. Snoeren, and Jennifer Yates. 2005. Cross-layer Visibility as a Service. In *HotNets*.
- [24] Hongqiang Harry Liu, Xin Wu, Ming Zhang, Lihua Yuan, Roger Wattenhofer, and David A. Maltz. 2013. zUpdate: Updating Data Center Networks with Zero Loss. In *SIGCOMM*.
- [25] Vincent Liu, Daniel Halperin, Arvind Krishnamurthy, and Thomas Anderson. 2013. F10: A Fault-Tolerant Engineered Network. In *NSDI*.
- [26] David Maltz. 2016. Keeping Cloud-Scale Networks Healthy. <https://video.mtgfs.com/video/4f277939-73f5-4ce8-aba1-3da70ec19345>. (2016).
- [27] Jitendra Padhye, Victor Firoiu, Don Towsley, and Jim Kurose. 1998. Modeling TCP Throughput: A Simple Model and Its Empirical Validation. In *SIGCOMM*.
- [28] Jonathan Perry, Amy Ousterhout, Hari Balakrishnan, Devavrat Shah, and Hans Fugal. 2014. Fastpass: A Centralized "Zero-queue" Datacenter Network. In *SIGCOMM*.
- [29] Peng Sun, Ratul Mahajan, Jennifer Rexford, Lihua Yuan, Ming Zhang, and Ahsan Arefin. 2014. A Network-state Management Service. In *SIGCOMM*.
- [30] USConec. 2017. Single Fiber Cleaning Tools. http://www.usconec.com/products/cleaning_tools/ibc_brand_cleaners_for_single_fiber_connections.htm. (2017).
- [31] Balaje Vamanan, Jahangir Hasan, and T.N. Vijaykumar. 2012. Deadline-aware Datacenter TCP (D2TCP). In *SIGCOMM*.
- [32] Christo Wilson, Hitesh Ballani, Thomas Karagiannis, and Ant Rowtron. 2011. Better Never Than Late: Meeting Deadlines in Datacenter Networks. In *SIGCOMM*.
- [33] Damon Wischik, Costin Raiciu, Adam Greenhalgh, and Mark Handley. 2011. Design, Implementation and Evaluation of Congestion Control for Multipath TCP. In *NSDI*.
- [34] Xin Wu, Daniel Turner, George Chen, Dave Maltz, Xiaowei Yang, Lihua Yuan, and Ming Zhang. 2012. NetPilot: Automating Datacenter Network Failure Mitigation. In *SIGCOMM*.
- [35] Kyriakos Zarifis, Rui Miao, Matt Calder, Ethan Katz-Bassett, Minlan Yu, and Jitendra Padhye. 2014. DIBS: Just-in-time Congestion Mitigation for Data Centers. In *EuroSys*.
- [36] Yibo Zhu, Haggai Eran, Daniel Firestone, Chuanxiong Guo, Marina Lipshteyn, Yehonatan Liron, Jitendra Padhye, Shachar Raindel, Mohamad Haj Yahia, and Ming Zhang. 2015. Congestion Control for Large-Scale RDMA Deployments. In

SIGCOMM.

- [37] Yibo Zhu, Nanxi Kang, Jiabin Cao, Albert Greenberg, Guohan Lu, Ratul Mahajan, Dave Maltz, Lihua Yuan, Ming Zhang, Ben Y. Zhao, and Haitao Zheng. 2015. Packet-Level Telemetry in Large Datacenter Networks. In *SIGCOMM*.
- [38] Danyang Zhuo, Monia Ghobadi, Ratul Mahajan, Amar Phanishayee, Xuan Kelvin Zou, Hang Guan, Arvind Krishnamurthy, and Thomas Anderson. 2017. RAIL: A Case for Redundant Arrays of Inexpensive Links in Data Center Networks. In *NSDI*.

A PROOF OF THEOREM 1

To prove Theorem 5.1, we first prove the following Lemma:

LEMMA A.1. *Let $N = (V, E)$ be a degraded Fat-Tree, where some links are turned off. Let $L \subseteq E$ be the set of enabled links with corruption. Finding a set $L' \subseteq L$ whose removal minimizes the impact of packet corruption s.t. all ToR switch pairs are still connected the the spine via valley-free routing after the removal of L' is NP-hard.*

PROOF. Our NP-hardness reduction is via the NP-complete problem 3-SAT, in the variant with exactly three literals per clause. Let I be an instance of 3-SAT [15], with k clauses C_1, \dots, C_k and variables x_1, \dots, x_r , $k \geq r$. We create an instance I' of our problem as follows: Consider a $4k$ -Fat-Tree, consisting of the three layers ToR, Agg, and the spine, where the Agg switches have $2k$ links down-and upwards, respectively. Pick one pod P with $2k$ ToR switches, C_1, \dots, C_k , corresponding to the clauses in I , and H_1, \dots, H_k , as helper switches, and lastly, $2r$ Agg switches $X_1, \neg X_1, \dots, X_r, \neg X_r$, corresponding to the possible literals in I , and, $2k - 2r \geq 0$ further Agg switches A_1, \dots, A_{2k-2r} . Let only the following three sets of links not be turned off in this pod P : 1) For each C_i , the links pointing to the Agg switches representing the corresponding literals contained in the clause in I , 2) for each H_j from H_1, \dots, H_k , one link each to $X_j, \neg X_j$, 3) for each H_{r+1}, \dots, H_k , one link each to $X_1, \neg X_1$. For the connection of the Agg switches in P to the neighboring spine switches, let only the following links L not be turned off, with $|L| = 2r$: From each Agg switch $X_1, \neg X_1, \dots, X_r, \neg X_r$ in P , one link to a neighboring spine switch. We set all links in L to have the same corruption properties greater than zero. The construction is illustrated in Figure 21.

To guarantee valley-free connection of all ToR switches in P to all other ToR switches in the other pods via the spine, each ToR switch C_i and H_j needs to have a connection to the spine, with the last part of each of those paths being a link from L . To maximize the set of links $L' \subseteq L$ that can be turned off, consider the following: First, for each pair of Agg switches $X_j, \neg X_j$, at least one needs to remain connected to the spine, or the ToR switch H_j would be disconnected (or for the case of $j = 1$, even more switches), meaning $|L'| \geq r$. Second, to connect each switch C_i to the spine, at least one its Agg switches (representing the literals of the clause) have to be connected to the spine. As thus, a solution to a satisfiable 3-SAT instance I tells us how to pick which of the links from each $X_i, \neg X_i$ pair should remain connected to the spine, and vice versa, a solution with $|L'| = r$ from I' shows how to satisfy I . On the other hand, should I not be satisfiable, then no solution with $|L'| \leq r$ can exist for I' , and vice versa as well. We note that the size of the instance I' is polynomial in k , i.e., we showed NP-hardness. \square

Since we assumed the same f_l on every link, I can be chosen arbitrarily, as long as $I(f_l) > 0$. We can now prove Theorem 5.1:

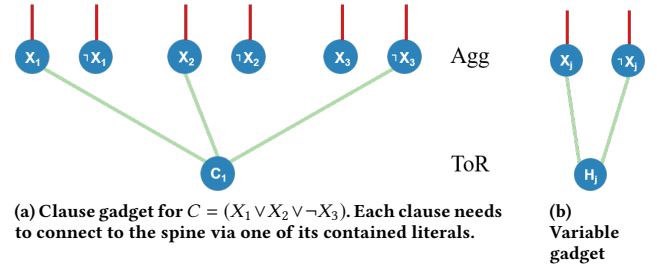


Figure 21: Reduction from 3-SAT: Each clause C is represented by a ToR switch, the literals X and $\neg X$ of each variable are represented by Agg switches. The ToR switches C are connected to the literals contained in their corresponding clause, cf. the clause gadget in 21a: Hence, at least one of the three literals needs to be connected to the spine. Each literal pair $X, \neg X$ is connected to at least one further ToR switch H , as shown in the variable gadget in 21b, ensuring that at least one literal of each variable is connected to the spine. The literals (Agg switches) only have one connection each to the spine, and all these connections are faulty, with the same error properties each. Finding a maximum set of these faulty links to turn off, s.t. all Tor switches still have valley-free connections to the remaining network, is NP-hard.

PROOF. Lemma A.1 assumed the network to be already degraded, i.e., some links \bar{L} are turned off. Note that a Fat-Tree is a special case of a Clos topology. We can extend the NP-hardness to the setting of Theorem 5.1 as well, by the following change in construction: Assume the errors on every link in \bar{L} are so high in comparison to the errors on the links from L , that for every link $l \in \bar{L}$ holds: Disabling l is more efficient regarding the impact of corruption than turning off *all* links in L . Lastly, to show that the underlying decision problem is in NP, observe that checking the capacity constraints and total impact of packet corruption of a given solution can be performed in polynomial time. \square

The above proof constructions can also be used as follows:

Optimizing for link removal. Another objective instead of total packet corruption could be the number of further links that can be removed. However, as all links in the proof of Lemma A.1 had the same error properties, NP-completeness still holds.

From ToR-spine connectivity to ToR-ToR connectivity. Lastly, in the above problem formulations, we wanted to maintain the ToR to spine connectivity of all ToR switches. However, we just considered a single pod P in each Fat-Tree construction, with the ToR switches in all other pods retaining all their connectivity to the spine. As thus, the above problems are also NP-complete for ToR-ToR connectivity, with the same proof constructions.